INTERNATIONAL JOURNAL OF CLIMATOLOGY
Int. J. Climatol. **25**: 1103–1125 (2005)
Published online in Wiley InterScience (www.interscience.wiley.com). DOI: 10.1002/joc.1157

CLOUD EFFECTS ON THE RADIATION BUDGET BASED ON ISCCP DATA (1991 TO 1995)

E. RASCHKE,[a,*] A. OHMURA,[b] W. B. ROSSOW,[c] B. E. CARLSON,[c] Y.-C. ZHANG,[d] C. STUBENRAUCH,[e] M. KOTTEK[f] and M. WILD[b]

[a] *Institut für Meteorologie, Universität Hamburg, Hamburg, Germany*
[b] *Institut für Atmosphäre und Klima, ETH Zürich, Zürich, Switzerland*
[c] *Goddard Institute for Space Studies, NASA, New York, USA*
[d] *Department Applied Physics and Mathematics, Columbia University, New York, USA*
[e] *Laboratoire de Météorologie Dynamique, Ecole Polytechnique, Palaiseau, France*
[f] *Dept. für Naturwissenschaften, Veterinär-Medizin. Universität Wien, Vienna Austria*

Received 9 July 2004
Revised 26 November 2004
Accepted 26 November 2004

ABSTRACT

Consistent and validated data sets of satellite-borne radiances and of a large variety of products describing the characteristics of terrestrial cloud and radiation fields have been produced within the International Satellite Cloud Climatology Project (ISCCP) covering the years 1983 through to 2003. A subset (annual and seasonal averages of the 5 year period 1991 to 1995) is used in this paper to discuss in greater detail the effect of clouds on the radiation fields at the upper and lower boundary of the atmosphere and in particular on the loss and gain (vertical divergence) of radiant energy by the atmosphere itself. Although this subset covers the effects of the Pinatubo eruption (June 1991) and of the strong El Niño event in 1992–93, which indeed caused 'anomalies in the average aerosol and cloud fields in the tropics and subtropics'. However, our regional averages of the radiation budget at the top of the atmosphere and at ground over a period of 5 years should be within 2–5 W m^{-2} of longer term averages.

We find very interesting spatial patterns in the global distributions of all quantities, which can be explained in part by various cloud field characteristics and by the continental surface characteristics. Most are known from similar studies with radiation budget measurements. Possibly for the first time, we show global fields of the vertical flux divergence of solar and terrestrial radiation within the atmosphere and of the effects of clouds. Both polar regions, various portions of China and the areas of persistent subtropical maritime stratocumulus fields over the Pacific and Atlantic Oceans and of cloud fields associated with the intertropical convergence zone (ITCZ) offer specific features for further analyses.

This ISCCP data set seems to underestimate the absorption of solar radiation in the tropical and subtropical atmosphere by about 10 to 20 W m^{-2}. There is a disagreement of about 30 W m^{-2} in global averages of the gain and loss of solar and terrestrial radiation in the atmosphere between this and two other independent data sets, which needs thorough investigation, since such data are required to validate the radiation budgets within circulation and climate models and for other climate studies. Such an assessment of radiation budget data is now under way within the auspices of the World Climate Research Programme. Copyright © 2005 Royal Meteorological Society.

KEY WORDS: climate; planetary radiation budget; satellites; clouds

1. INTRODUCTION

Clouds within the atmosphere play a vital role in a large and complex variety of physical and chemical processes that determine our climate and also cause various feedbacks. They result from many internal processes within the atmosphere and exchanges with the surface, but they also influence both with their own characteristics. Clouds are the source of precipitation. They interact with aerosols and the electric and

* Correspondence to: E. Raschke, Institüt für Meteorologie, Universität Hamburg, Bundesstrasse 55, 20146 Hamburg, Germany; e-mail: raschke@dkrz.de

radiation fields in the atmosphere, and they interact with atmospheric dynamics. We focus in this paper on the contributions of clouds to up- and downward fluxes of solar and terrestrial radiation at both boundaries of the atmosphere and, consequently, also on the vertical radiative flux divergence within the atmosphere.

It always has been a goal of the geo-sciences to determine and predict quantitatively and precisely the abundance and location of cloud fields, their composition of ice and water, their total water content, their radiative characteristics and the mutual interactions between those characteristics and atmospheric dynamics. Many of these characteristics can now be estimated with reasonable precision from recent multi-spectral satellite measurements over all regions of the Earth, whereas predictions in global and regional numerical models of the circulation within the climate system are still quite uncertain (Gates *et al*., 1999; Betts and Beljaars, 2003; Covey *et al*., 2003).

Many open questions on the processes and participating agents determining various cloud characteristics can now be answered by numerical simulations using cloud resolving models (Randall *et al*., 2003) and with data sets gathered during airborne campaigns (e.g. the European project EUCREX (Raschke *et al*., 1998) or the project ARESE (Valero *et al*., 2003)) or by relevant analyses of satellite data. The *in situ* measurements also collect valuable data for the validation of remote-sensing methods to be applied to more recent advanced satellite data sets.

The International Satellite Cloud Climatology Project (ISCCP; Schiffer and Rossow, 1983) was designed during the early 1980s to provide global information on cloud fields as they could be described at that time by available operational weather satellite cloud imaging data (Schiffer and Rossow, 1985). This cloud data set now covers a period of two complete decades, starting in 1983. It has been used together with a large variety of other data on the concurrent status of the atmosphere and surface to compute the radiation budget parameters at the top of the atmosphere and at the ground. The results shown here are the final product of earlier work and sensitivity studies (Rossow and Zhang, 1995; Zhang *et al*., 1995, 2004). These results are called the ISCCP-FD data set, where the acronym FD (for flux data) stands for a more recent version of ISCCP data set. In parallel with the ISCCP, other projects determine cloud and radiation budget parameters from combinations of satellite data, such as now provided by the Clouds and the Earth's Radiant Energy System (CERES; Wielicki *et al*., 1996) and other complementary information on the state of the atmosphere, and the surface as well.

It is the purpose of this paper to describe briefly some details in annual mean radiation fields that were obtained from a selected subset of the ISCCP-FD data set, which covers the 5 year period from January 1991 to December 1995. A longer time series is now available, but needs thorough assessment. We show here, possibly for the first time, global maps of the radiative heating or cooling of the atmosphere (which corresponds to the 'classical' radiative flux divergence in vertical atmospheric columns) and of the cloud effects on them. Also, the uncertainty limits are discussed. In the discussion of various quantities we pay special attention to the cloud and radiation fields over several specific regions: China, the intertropical convergence zone (ITCZ), mid-latitude storm tracks, subtropical maritime stratocumulus over both oceans and both polar regions. Details of the seasonal variability will be the subject of a separate consideration.

2. ISCCP DATA SETS

The radiance data from imaging passive radiometers onboard operational polar orbiting and geostationary meteorological satellites are continuously collected and calibrated to remove instrumental drifts, uncertainties in individual calibration histories, the satellite-to-satellite changes of spectral sensitivity and other unforeseen problems. The calibration procedure requires careful intercomparison of collocated and nearly simultaneous measurements from different satellites and also comparison with other ground-based and airborne measurements over selected areas. Details of this procedure are described in Brest and Rossow (1992), Desormeaux *et al*. (1993) and Brest *et al*. (1997), where estimates of uncertainty ranges are also given.

The present estimates are an absolute (relative) uncertainty of less than 7% (3%) for radiances in the visible (solar) spectral range and of 2% (1%) for the infrared (terrestrial) radiation. These data form a time series covering all years since July 1983 to now, available at a spatial sampling interval of 30 km and a time interval

Table I. Data sets used in cloud retrievals and in the calculation of radiative fluxes. Unless noted otherwise, each data set provides a record of the variable covering the specific years of the calculations

Variables	Data sources for these variables
Cloud cover, optical thickness, top temperature by type	**ISCCP satellite radiances**
Cloud particle size	ISCCP-based climatology
Cloud vertical structure	Combined ISCCP–rawinsonde climatology
Atmospheric temperature and tropospheric humidity	TOVS, Oort climatology for filling
Atmospheric humidity (upper troposphere, stratosphere)	SAGE climatology
Atmospheric composition	Actual record from various sources
Stratospheric total ozone	TOMS, TOVS for filling
Stratospheric ozone profiles	SAGE climatology
Stratospheric aerosols	SAGE
Tropospheric aerosols	Baseline current-day climatology
Snow cover	NOAA product
Sea ice cover	NSIDC product
Diurnal cycle of air temperature over land	Climatology based on surface weather reports and NCEP reanalysis
Surface skin temperature and visible reflectance	From ISCCP retrievals
Surface spectral albedo and emissivity by type	Goddard Institute of Space Studies (GISS) general circulation model reconstruction by surface type and season

of 3 h. The cloud products are available at 30 km and 3 h (called DX data), 280 km and 3 h (called D1 data) and 280 km and monthly (called D2 data). Information on how to obtain the six ISCCP data products (satellite radiances, atmospheric temperature and humidity, snow/ice, three cloud products), together with the radiative flux products and other correlative data discussed here (see Table I), can be found at http://isccp.giss.nasa.gov (and Rossow and Duenas, 2004).

For the derivation of cloud properties and radiation fields in the atmosphere, the data are sampled randomly at intervals of about 30 km to reduce the computational requirements to a manageable size. Sampling studies have shown that this random sampling preserves all larger scale information on cloud and radiation fields quite accurately (Seze and Rossow, 1991). The radiative fluxes are calculated at 280 km and 3 h intervals based on the cloud type information in the ISCCP D1 data set.

3. CLOUDS

To resolve the diurnal cycle of clouds, ISCCP emphasizes temporal and spatial resolution, rather than spectral resolution. To achieve global coverage, the only possibility was to use the measurements of reflected solar radiation during the daylight period and of the heat radiation in the infrared (IR) atmospheric window that are common to the imagers on the suite of operational geostationary and polar orbiting weather satellites. Time sampling is every 3 h and the initial spatial resolution of about 5 km is randomly sampled at about 30 km. Clouds are detected through a variable threshold test, which compares the measured radiances to 'clear-sky composite' radiances that have been inferred from a series of statistical tests on the space and time variations of both spectral radiances (Rossow and Garder, 1993). Clear sky conditions are associated with spatial and temporal variability of the atmosphere and surface, that is usually lower than for cloudy scenes and that is regionally dependent.

ISCCP cloud properties are determined by comparing the observed radiances with a detailed radiative transfer model. The model includes effects of the atmosphere, with properties specified from the operational

TIROS Operational Vertical Sounder (TOVS) data analysis, and effects of the surface determined from the clear radiances. Cloud-top temperature is first retrieved assuming that all clouds are opaque (i.e. black bodies). During daytime, when solar radiances are available to retrieve solar cloud optical thicknesses τ, the cloud-top temperature of 'transmissive' clouds ($\tau < 5$) is corrected to account for the radiation transmitted from below. Cloud-top temperature is then converted into cloud-top pressure using operational TOVS atmospheric profiles. Ice and water clouds are distinguished by a cloud-top temperature of 260 K. Water clouds are assumed to be composed, on average, of 10 μm radius spherical liquid water droplets; ice clouds are treated with a model cloud composed of 30 μm ice poly-crystals. Liquid and ice water paths (LWP, IWP) are estimated from the cloud optical thickness, using the same assumptions of effective particle size as in the radiative transfer model (Rossow and Schiffer, 1991; Rossow *et al*., 1996; Rossow and Schiffer, 1999).

The global pattern of the 5-year annual mean of cloud cover is shown in Figure 1. Tables II and III summarize global averages compared with results from the TOVS path-B data set (Scott *et al*., 1999; Stubenrauch *et al*., 1999a) for nearly the same period. A detailed description of diurnal, seasonal and interannual variations of cloud properties, as well as a discussion of uncertainties, is given in Rossow and Schiffer (1999). Note in particular the pattern over the Indian Ocean. It is caused by a gap in the areal

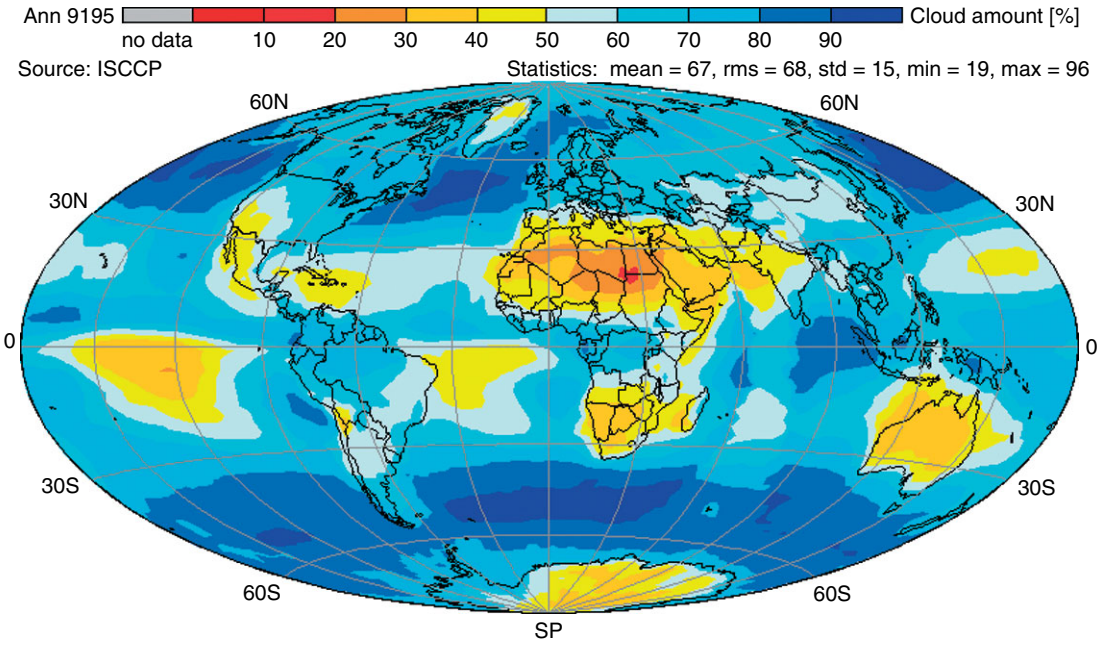

Figure 1. Annual average total cloud amount over the Earth (period 1991 to 1995) derived from the ISCCP data sets

Table II. Global cloud properties from 5 years of ISCCP/TOVS path-B (italic)

Quantity	Global		Ocean		Land	
Cloud amount (%)	67	*73*	71	*75*	57	*69*
Cloud-top temperature (K)	261	*261*	266	*264*	251	*256*
Cloud-top pressure (hPa)	587	*607*	631	*631*	489	*547*
Cloud optical thickness	4.2		4.2		4.1	
Effective emissivity	*0.57*		*0.57*		*0.55*	
Cloud water path (g m^{-2})	62.0		58.6		69.6	
Atmospheric water vapour (cm w.e.)	*2.51*		*2.60*		*2.23*	

Table III. Global cloud-type amounts from 5 years ISCCP and TOVS path-B (italic)

Cloud type	Amount (%)					
	Global		Ocean		Land	
Deep convection	2.8	*2.4*	2.8	*1.9*	2.7	*3.5*
Cirrus	5.9	*13.8*	6.1	*13.7*	5.5	*13.9*
Thin cirrus	12.8	*13.3*	11.5	*13.2*	16.0	*13.6*
Nimbostratus	2.0		1.7		2.7	
Altostratus	7.4	*8.5*	7.3	*7.2*	7.7	*11.7*
Altocumulus	9.0	*3.5*	9.3	*3.0*	8.1	*4.9*
Stratus	1.6		1.6		1.6	
Stratocumulus	12.1	*19.1*	14.1	*21.5*	7.6	*12.7*
Cumulus	13.0	*12.6*	15.0	*14.4*	8.3	*8.1*

coverage over the central portion of the Indian Ocean and over India between the geostationary satellites Meteosat (from Europe) and GMS (from Japan). The discontinuities are produced by a dependence of the ISCCP retrievals on satellite view angles (Rossow and Garder, 1993), which changes dramatically. But the respective changes in optical thickness and cloud-top temperature also compensate this error in computations of the radiation field almost completely. This area in more recent data sets is covered by observations of the satellite Meteosat 5.

The pattern of clouds in Figure 1 reflects the known pattern of the mean annual atmospheric circulation (e.g. Peixoto and Oort, 1992). For further discussion of results we point here to specific cloud fields over the ITCZ, over China (Yu *et al*., 2004), the subtropical maritime stratocumulus near the western coastal zones of Africa and the Americas and the major cyclone tracks in the mid-latitudes of both hemispheres, where high cloud amounts of 70% are observed. Over both polar regions the identification of clouds in passive measurements from satellites is extremely difficult, and related results should be considered with due caution.

Tables II and III compare the global averages of cloud properties which are independently obtained from the ISCCP data set and from the TOVS path-B data set (Smith *et al*., 1979). Clouds cover about 70% of the Earth's surface, where about 5–10% more cloudiness over ocean is found in both analyses than over land. The average cloud-top temperature is about 261 K. Clouds in these analyses are generally found lower and optically thicker over ocean than over land, possibly also due to the relative stable background temperatures and albedos of the ocean. All averages are determined from areal means covering an area of about 280×280 km^2. Note, that more clouds, but also somewhat 'warmer' clouds, are found in both data sets over the oceans than over the continents, possibly due to the more accurate knowledge of ocean surface temperatures, but also due to different convective forcings over the two surfaces. The TOVS procedure seems to find more clouds than the ISCCP, since it is a little more sensitive to thinner clouds (Stubenrauch *et al*., 1999b).

It is interesting to note that the global averages from ISCCP and TOVS path-B agree very well, even if they have been obtained from different instruments and time series. If one is interested in changes of cloud properties (seasonal or interannual), then these cannot be adequately described by an average and standard deviation of cloud properties, but must rather be described by correlated changes in several cloud properties or changes in cloud-type amounts (Rossow and Cairns, 1995).

Notable limitations of the ISCCP cloud data sets are summarized in Rossow and Schiffer (1999): (1) About 5–10% areal coverage by isolated cirrus with optical thicknesses less than about 0.3 are not detected by ISCCP. Tests of the radiative effects by Chen and Rossow (2002) show that this does not affect the results by more than 1–2 W m^{-2}. (2) ISCCP cloud detections are less reliable in the polar regions, where it appears that the ISCCP cloud amounts are underestimated, particularly in summertime. (3) Multi-layered clouds are misidentified as middle-level clouds when the uppermost layer is optically thin, which appears to happen about 15–25% of the time. This causes some bias in the terrestrial radiation fluxes (Chen and Rossow, 2002).

Adjustments have been made in the input cloud parameters for the FD data set that partially compensate for the last two limitations.

Both data sets in Table III show similar results for cloud types, except for the cirrus, altocumulus and stratocumulus. This disagreement of the net amounts of cirrus and altocumulus indicates different height assignments for optically thin clouds. The disagreement for stratocumulus indicates different detection sensitivities for low clouds. Systematic differences can be observed over layered (TOVS > ISCCP) and convective (TOVS < ISCCP) cloud fields. Since the spectral TOVS radiances allow for a better resolution of cloud patterns in the middle and upper troposphere, these data are more sensitive to upper cirrus, whereas altocumulus might be underestimated. On the other hand, the TOVS radiances are less discriminating for low clouds. But the discrepancies between these results are also due to different sampling in space and time and to different analysis techniques. The upcoming new and spectrally, as well as spatially, more highly resolved measurements from both geostationary and polar orbiting operational satellites might be better suited for this purpose.

If one considers the distribution of cloud types in Table III, the instruments that were used for the observations play an important role. According to the present ISCCP results, the globe is covered by about 22% high, 18% mid-level and 27% low clouds; TOVS path-B reports 30%, 12% and 32% respectively. The higher spectral resolution of the vertical IR sounder is better suited to identify high semi-transparent clouds (e.g. Jin *et al*., 1996; Stubenrauch *et al*., 1999b; Wylie and Menzel, 1999). However, both data sets agree on a higher occurrence of low clouds over ocean and of high clouds over land. Both climatologies give information only on the uppermost clouds in each column. Long-term information on the vertical structure of clouds is only available so far by using a collection of rawinsonde measurements (Wang *et al*., 2000).

In summary, we must accept the following limitations within this cloud data set: these are results on cloud fields that are derived from passive radiance measurements made primarily only in two spectral intervals, where (1) over cold ice/snow-covered regions, since the radiance contrast between clear sky and cloudy sky is often very small, this method will have more difficulty deriving cloud properties, and (2) where the top-down view prevents detection of clouds at lower levels if they are masked by clouds aloft.

More can be learned by a combined analysis of multi-spectral imaging and IR sounding instruments and of visible–IR and microwave imaging instruments, but more significant improvements are expected from the future flight of active cloud sensors on satellites, both lidar and cloud radar (e.g. Stephens *et al*., 2002), which will be available in addition to the satellite imaging data. The lidar data of the satellite ICESat (Mahesh *et al*., 2004) already provides valuable information on the location of cirrus and aerosol layers in the atmosphere.

4. RADIATION BUDGET COMPONENTS AND CLOUD EFFECTS

All radiation budget quantities have been computed using as input the above-mentioned correlative and cloud data (see Table I). The radiative transfer code is the same as used in the present climate model of the GISS (e.g. see Zhang *et al*. (1995, 2004)). In order to reduce the computational effort, the calculations are performed for areas of about 2.5° latitude–longitude in size; however, the effects of different cloud types, defined by their top pressure and optical thickness, are calculated explicitly. In this procedure, computations at each grid area were made independently for clear and cloudy skies during each time step, where the respective cloud field characteristics are derived from the ISCCP radiance data (see Section 3). These 3 h values are integrated to daily sums and to other time averages.

The ‘cloud effect’ on radiant energy fluxes is represented simply by the difference between fluxes for cloudy and clear skies. These values are positive (negative) when clouds increase (decrease) the respective flux. These quantities are also called ‘cloud radiative forcing’ (CRF). We adopt the following convention of signs: All downward (upward) fluxes are counted positive (negative). Positive (negative) values of the vertical divergence of radiant energy, since they are computed as differences between net fields at the top of the atmosphere (TOA) and at the surface, mean a net gain (loss) of radiant energy by the atmosphere.

For the ISCCP-FD data set, the clear-sky fluxes are calculated for all scenes, whether cloudy or clear. Thus, they represent a different statistical sample of the atmosphere than (for example) in the CERES or

Earth Radiation Budget Experiment (ERBE) data (e.g. Wielicki *et al*., 1996). Also, in the ISCCP-FD data set, when clouds are added to the atmosphere, layer humidity is increased, usually by about 5–10%, to saturation, so that the total water vapour amount for cloudy fluxes differs from the clear-sky amount; the effect of the added water vapour is included in the cloud effects shown here. Further, the actual and highly variable amount of aerosols is not considered here, since it is not yet known or available. Significant changes in clear-sky fluxes of solar radiation, and to some extent also of terrestrial radiation, may therefore occur due to additional anthropogenic (biomass burning) and natural (e.g. dust storms, volcanoes) aerosols, which are not considered in the climatological aerosols (Table I) used in the ISCCP flux calculations. However, variations in stratospheric aerosol caused by volcanoes are accounted for using results from SAGE (Table I).

4.1. Radiation budget at the TOA

Assuming a constant total solar irradiance of 1367 W m^{-2}, and taking all atmospheric characteristics from the summary in Table I, the following radiation fields have been calculated for the cloud-free and cloudy atmosphere at the TOA and at ground: incoming and reflected solar radiation, and the emitted terrestrial radiation.

Validation of the results at the TOA is possible by comparison with results of other, more direct determinations from specific satellite radiation flux experiments, such as the ERBE and CERES (Barkstrom, 1984; Wielicki *et al*., 1995, 1996), where the upward broadband radiances are measured directly with radiometers. An example is shown in Figure 2. The differences between the two data sets over most regions of the globe range between about ±10 and 15 W m^{-2}, leaving open the question of which data set is the best. The CERES clear-sky data over oceans show some effects of thin cloud contamination. CERES data for cloudy (i.e. all-sky) conditions are up to 30 W m^{-2} higher than those of the ISCCP-FD. The banded

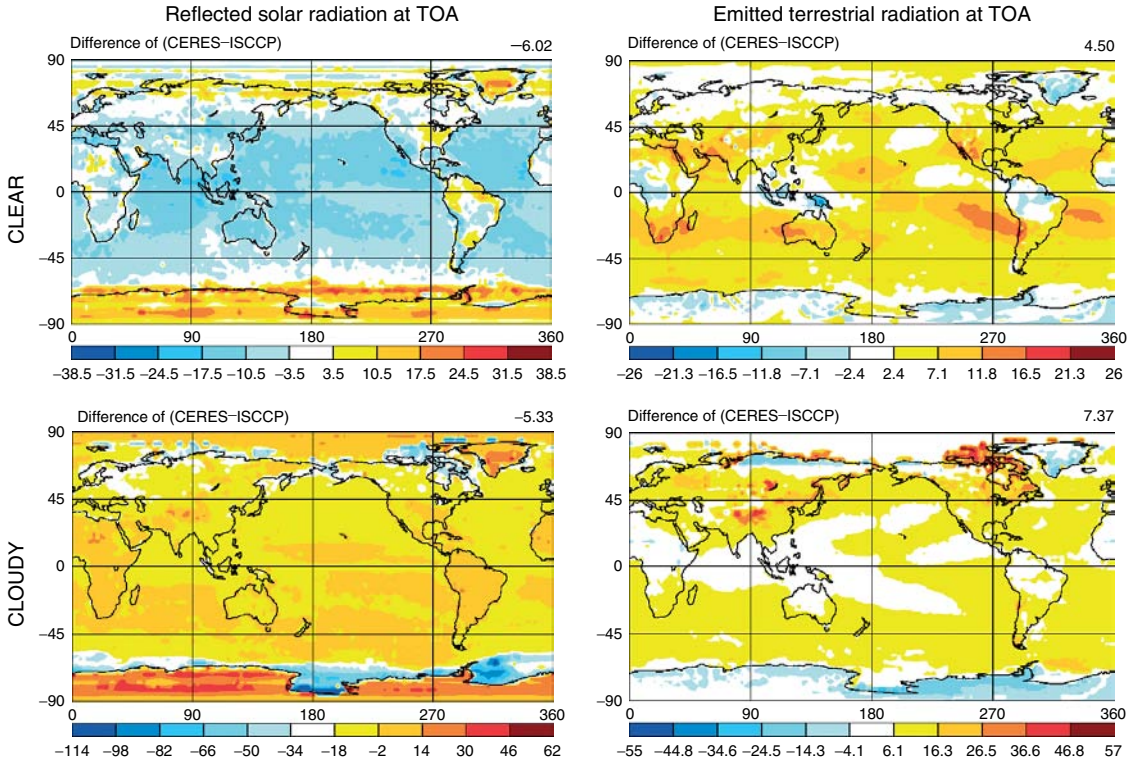

Figure 2. Differences between annual averages of reflected (left panels) solar radiation and emitted terrestrial (right panels) radiation for clear skies (top panels) and for all situations (lower panels) at the TOA during the period July 2000 to June 2001, which were computed from the CERES and ISCCP data sets. These differences illustrate the uncertainty ranges in such data and suggest their possible causes

structures in the left panels are due to data areal mismatches and possibly to different corrections of angular dependence. There seems to be a small difference in the surface albedo of the arctic ice in both data sets.

Note that the clear-sky fluxes are determined from the two data sets in different ways. For the ISCCP data they are directly computed, whereas for the CERES data the clear-sky fluxes are averaged over scenes determined to be clear by various thresholds. A study by Hartmann and Doelling (1991) has shown that this latter approach tends to slightly underestimate (overestimate) the reflected solar (emitted terrestrial) fluxes for clear skies. This effect may also contribute to the cloudy difference pattern in Figure 2 (lower panels). Direct intercomparison with well-calibrated airborne measurements is also possible over scenes, which are very uniform within the hemispheric field of view of high-altitude (around 13–15 km) aircraft; however, the reflection and emission of radiation in all atmospheric layers above the aircraft must be calculated from relevant data. Such specific measurements have not yet been done. They require carefully calibrated equipment, whose performance is not altered in flight.

As an example for all other more specific and detailed products we show in Figures 3(a) and (b) the maps of the annual average of the net radiation and of the cloud effects on it. These maps show patterns that are

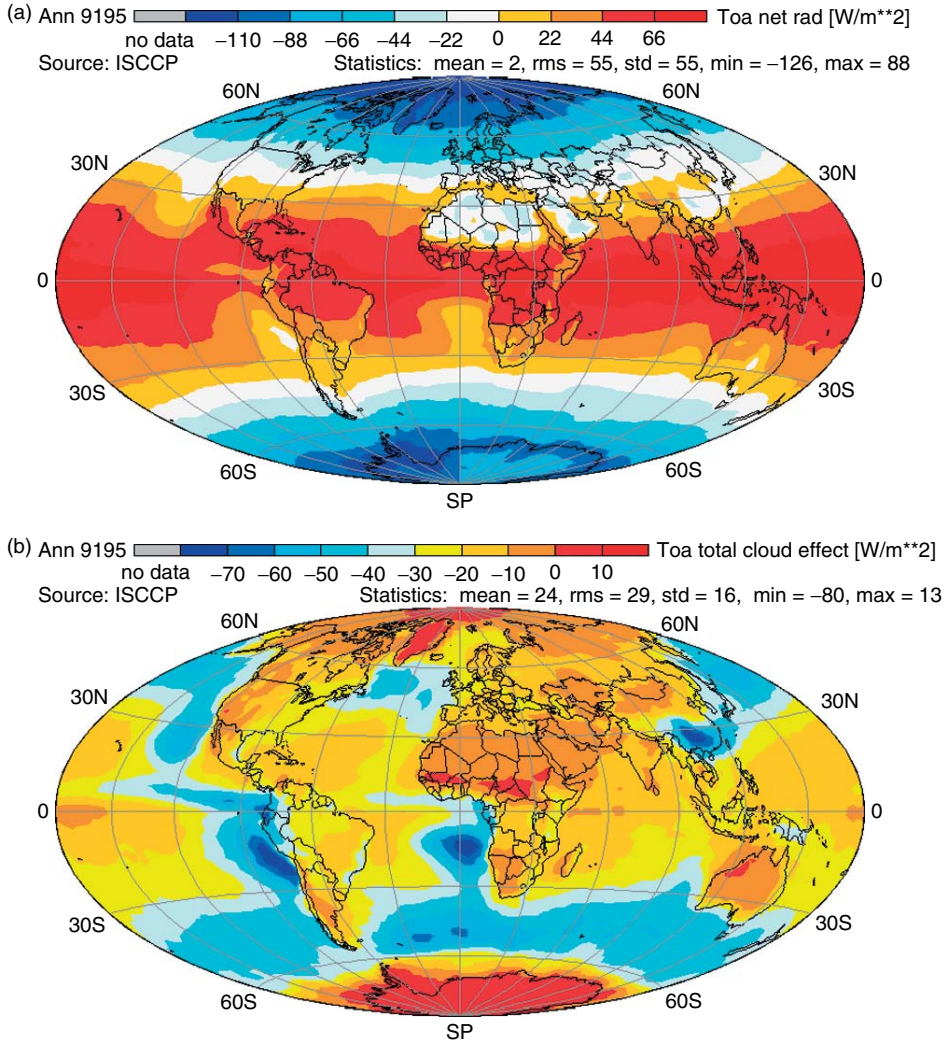

Figure 3. (a) Net radiation budget at the TOA and (b) the cloud effect (cloudy minus clear) on it (period: 1991–95). Negative values in the lower map mean that clouds generally reduce the net radiation, thus they are cooling the planet

very similar to maps for the same quantities, but which are derived from other measurements. The general patterns and amounts in Figure 3(a) (net radiation at TOA) agree quite well with many earlier results, even with those obtained from the 'historical' satellites of the Nimbus series (e.g. Raschke, 1972), where already the deficit anomalies over the African and Arabian deserts were identified.

Clouds, as can be seen in Figure 3(b), seem to increase slightly (up to 10 W m^{-2}) the net radiation at the TOA over both polar regions and over northwest Australia and over West and Central Africa (or decrease the cooling to space). Over these latter regions the absolute values of the cloud effect on the net budgets of solar and terrestrial radiation at the TOA amount to about 40 W m^{-2}, but they almost cancel each other in the total budget due to their opposite signs.

The positive values of the cloud effects in the polar regions of about 8 to 12 W m^{-2} may result from a dominance of the cloud effects on terrestrial radiation at the TOA, which are apparently in the average a bit warmer and reduce the cooling of the colder surface. This is because the cloud effects on solar radiation are reduced both by the large surface albedo values and the lack of sunlight during a large part of the year. We are aware of the fact that optically thin clouds in particular are difficult to measure with the ISCCP procedure. A similar effect is produced by optically thin cirrus clouds over several areas in Australia, Africa and Asia.

Over all other regions, clouds decrease the net radiation at the TOA due to a combined effect of reflection of solar radiation and emission of terrestrial radiation. Note that the strongest reduction of the net radiation is due to the persistent low (and, therefore, warm) maritime stratocumulus decks along the western coastal zones of the Americas and of Africa.

A similar anomaly is found over southern China, where Figure 1 shows a cloud amount of more than 70%. Here, in the annual average, mid-level clouds dominate and reduce the net budget by more than 70 W m^{-2}. This anomaly over China is also visible in the maps of cloud effects on net solar (-100 W m^{-2}) and net terrestrial ($+25-30$ W m^{-2}) radiation at the TOA.

4.2. Radiation budget at the surface

The radiation budget at the surface controls many immediate dynamic processes in the atmospheric boundary layer and the heat storage in upper ocean and soil layers. Therefore, extended ground-based networks for the monitoring of downward fluxes of solar radiation, and to a lesser extent of atmospheric (terrestrial or thermal) radiation, were previously established by various national weather and climate services, which were often complemented by networks of other environmental services. There are numerous earlier estimates available made on the basis of measurements and climate data. Many attempts in past years to estimate the surface radiation budget from operational satellite data culminated in various algorithms which are now applied both operationally and experimentally. The World Climate Research Programme encouraged several nations to maintain one or more special stations with quite sophisticated and high-quality equipment, forming the Baseline Surface Radiation Network (BSRN; Ohmura *et al.*, 1998), which is now consisting of 35 stations. These are located in most climate regions of the Earth. More data (primarily solar data) from operational networks is available from the Global Energy Budget Archive (GEBA; Gilgen and Ohmura, 1997). However, such measurements are not available over the open oceans and over larger lakes, except from a very few small islands, experimental ships and buoys. Measurements of the upward components of the radiation budget at the ground make no sense for our purposes, since they only represent very local conditions, although they are done at many stations.

In Figure 4 we compare monthly averages of measured and computed downward fluxes as obtained for various *individual* BSRN stations. Unfortunately, in all cases shown there was no access to BSRN measurements during the full period, 1991–95. From this intercomparison we can observe some bias of the ISCCP-FD results, in particular for small values. In some cases there is more noticeable scattering. Some of these problems may be associated with the fact that the individual stations may not be representative of the larger averaging area (about 280×280 km^2) of the ISCCP data, but some of these problems can also be explained by the cloud sampling (see further details in Rossow and Zhang (1995)) and the atmospheric and surface properties of the ISCCP (see Table I). Therefore, we recommend repeating such comparisons with the data sets of the 'best-suited' national or regional station clusters as they exist over several areas of all continents (e.g. the GEWEX Continental Scale Experiment regions).

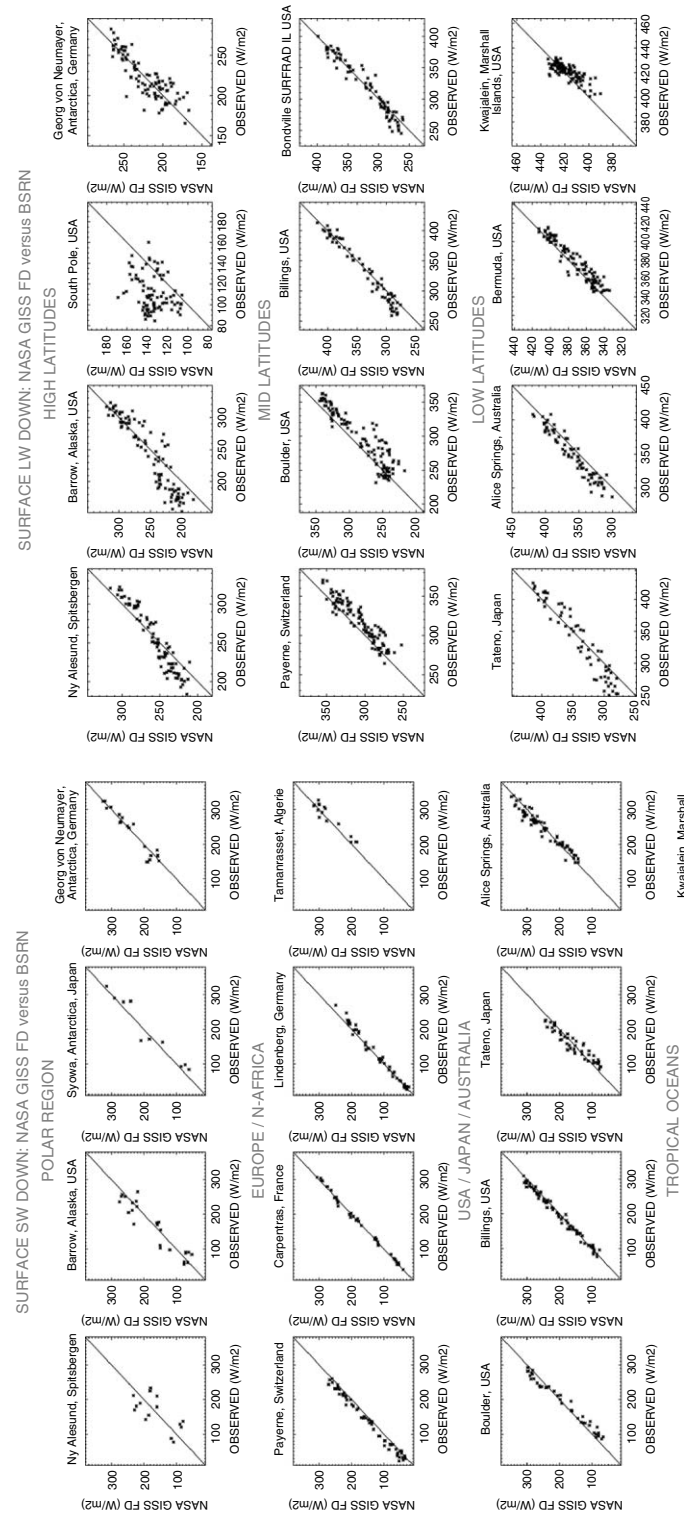

Figure 4. Comparison of monthly areal average (280 × 280 km^2) downward solar radiation (a) and downward atmospheric radiation (b) from the ISCCP-FD data set (ordinate) with point measurements at various BSRN stations. Note the larger discrepancies at high latitudes, which might be due to errors in air temperatures and cloud base heights, but may also indicate problems with the pyrgeometers at these low temperatures

The downward solar radiation might be, as seen in the left portion of Figure 4, slightly overestimated by the ISCCP algorithm at most stations at low and middle latitudes. This may be associated with an underestimate of absorbing aerosols from biomass burning in tropical areas and may alter the very small contributions of clouds to the absorption of solar radiation in the atmosphere, as shown in Figure 7(a). In the IR (terrestrial radiation) the scatter of data on the downward fluxes is very high at near-polar stations, possibly due to errors in the atmospheric data and errors in the measurements. In part, ISCCP seems to overestimate this quantity systematically at low temperatures because of systematic errors in the TOVS representation of situations with near-surface temperature inversions. At lower latitudes there is a tendency for the ISCCP model to underestimate the downward atmospheric radiation at higher intensities and overestimate it at lower intensities. This may also be caused by small, but systematic, errors in the TOVS temperature profiles near the surface (Stubenrauch *et al.*, 1999a).

In the remaining part of this section we discuss the fields of downward solar and terrestrial radiation and the clouds effect on them in some detail (see Figures 5 to 7), since they are of particular interest not only for climate studies, but also in various other applications (e.g. design of installations to produce renewable energy).

Instead of a map for the downward solar radiation, we show in Figure 5 a map of its amount as related to the annual solar influx at the TOA. These values can be interpreted as an "effective transmittance" of the atmosphere for solar radiation. Here a value of unity would mean the total absence of the atmosphere. The largest reductions occur over the cloudy regions of mid-latitudinal storm tracks, whose effective transmittance is persistently below about 0.42. Somewhat less, but significant, reductions can be observed over the aforementioned areas over China, with an effective transmittance as low as about 0.42 to 0.48, and over the subtropical maritime cloud fields, with values between about 0.48 and 0.54. Areas of larger transparencies of more than 0.6 over the continents reflect also various topographic features, and also the general pattern of atmospheric circulation. Over the Sahara and eastern near-equatorial Pacific Ocean more than about 0.66 of the incident radiation reaches the ground.

In Figure 6(a) and (b) we compare the fields of downward terrestrial (atmospheric) radiation and of the related contributions by clouds. The mean downward atmospheric radiation field (Figure 6(a)) is dominated

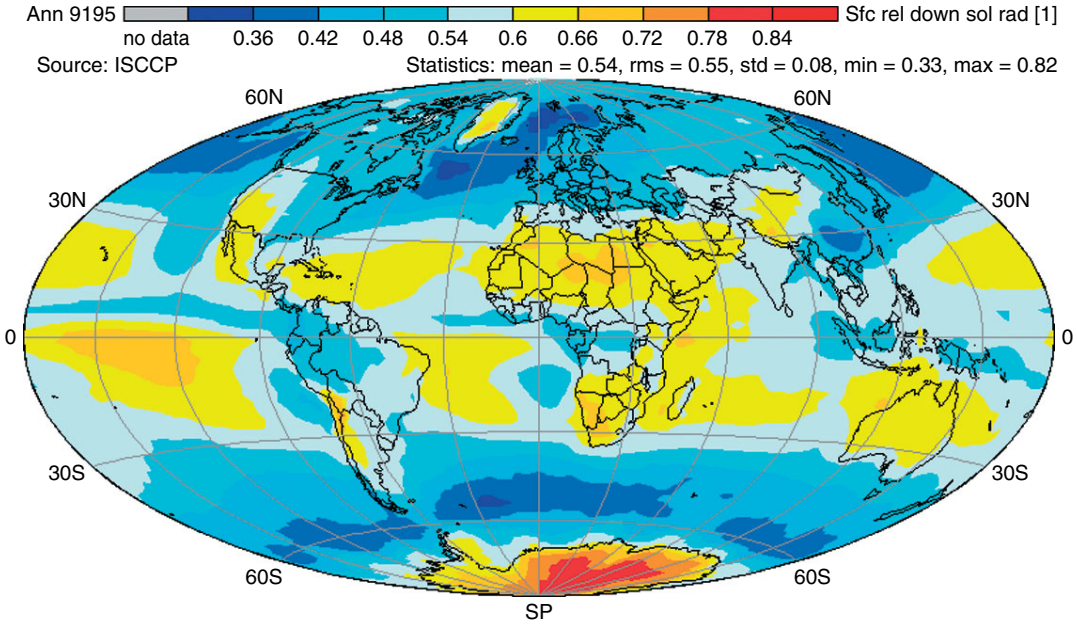

Figure 5. Downward solar radiation at the ground as a fraction of the incoming at TOA flux. These values of the effective transmittance of the atmosphere for solar radiation already provide an impression of the effect of clouds and of elevation of some continental areas. Note the very low values over China, due to clouds, and over the major storm tracks in both hemispheres

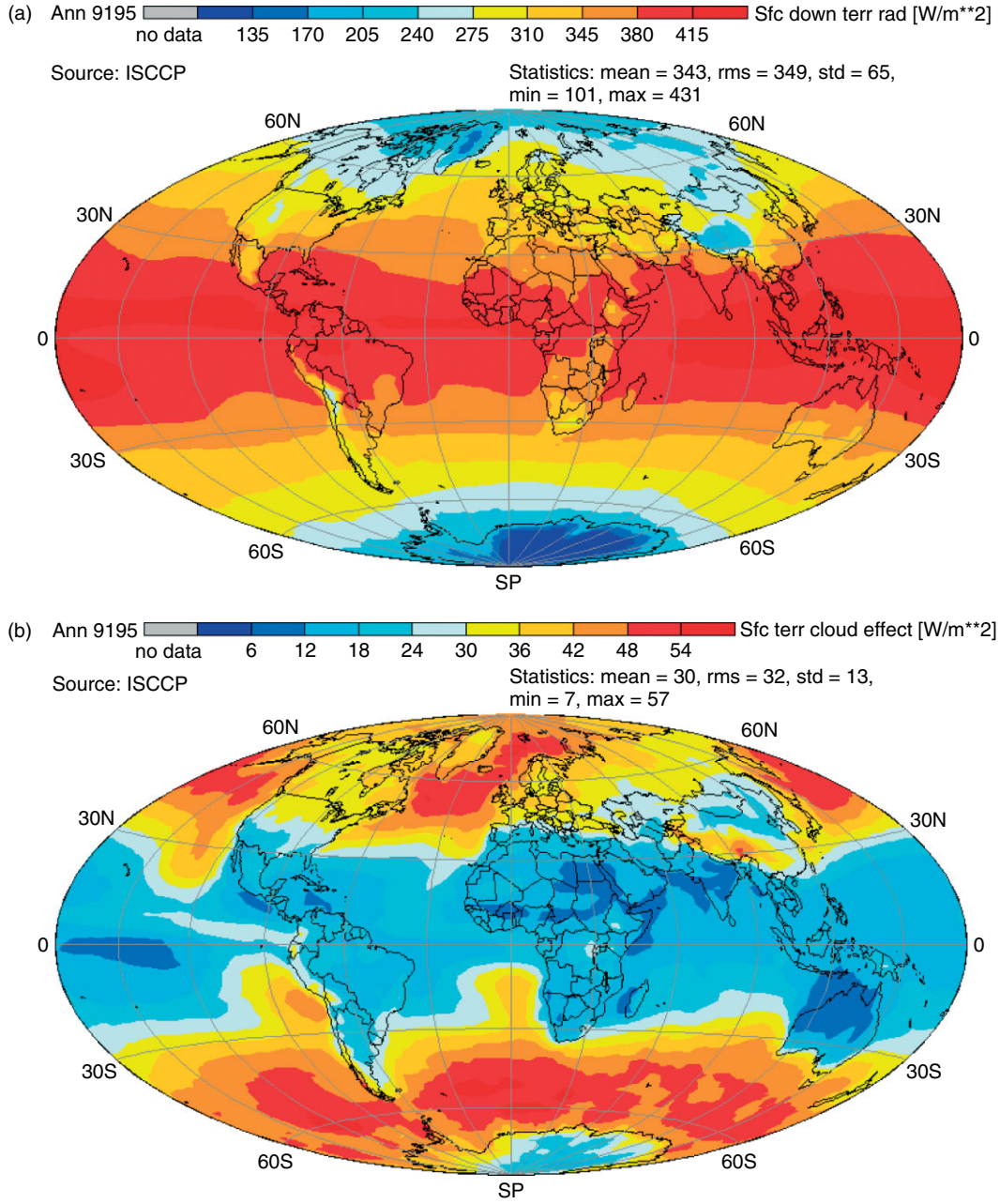

Figure 6. (a) Downward terrestrial radiation (W m^{-2}) at ground and (b) effects of clouds (cloudy–clear) on downward terrestrial radiation (W m^{-2}) during the period 1991 to 1995. This cloud effect is generally positive over all areas, since clouds enhance the downward atmospheric radiation

by the mean temperature and water vapour content of the lower atmosphere near the surface. Only a few continental areas with low humidity and with higher elevations cause zonal anomalies in this general pattern.

The major cloud contribution, often of more than +42 W m^{-2}, is concentrated in areas of the major mid-latitude storm tracks over both hemispheres. A small but significant maximum occurs westward of the 'anomaly over southern China' at the southern edge of the Highland of Tibet, with values between about 36 and 48 W m^{-2}. This maximum also occurs as a significant regional anomaly of high absorption of solar

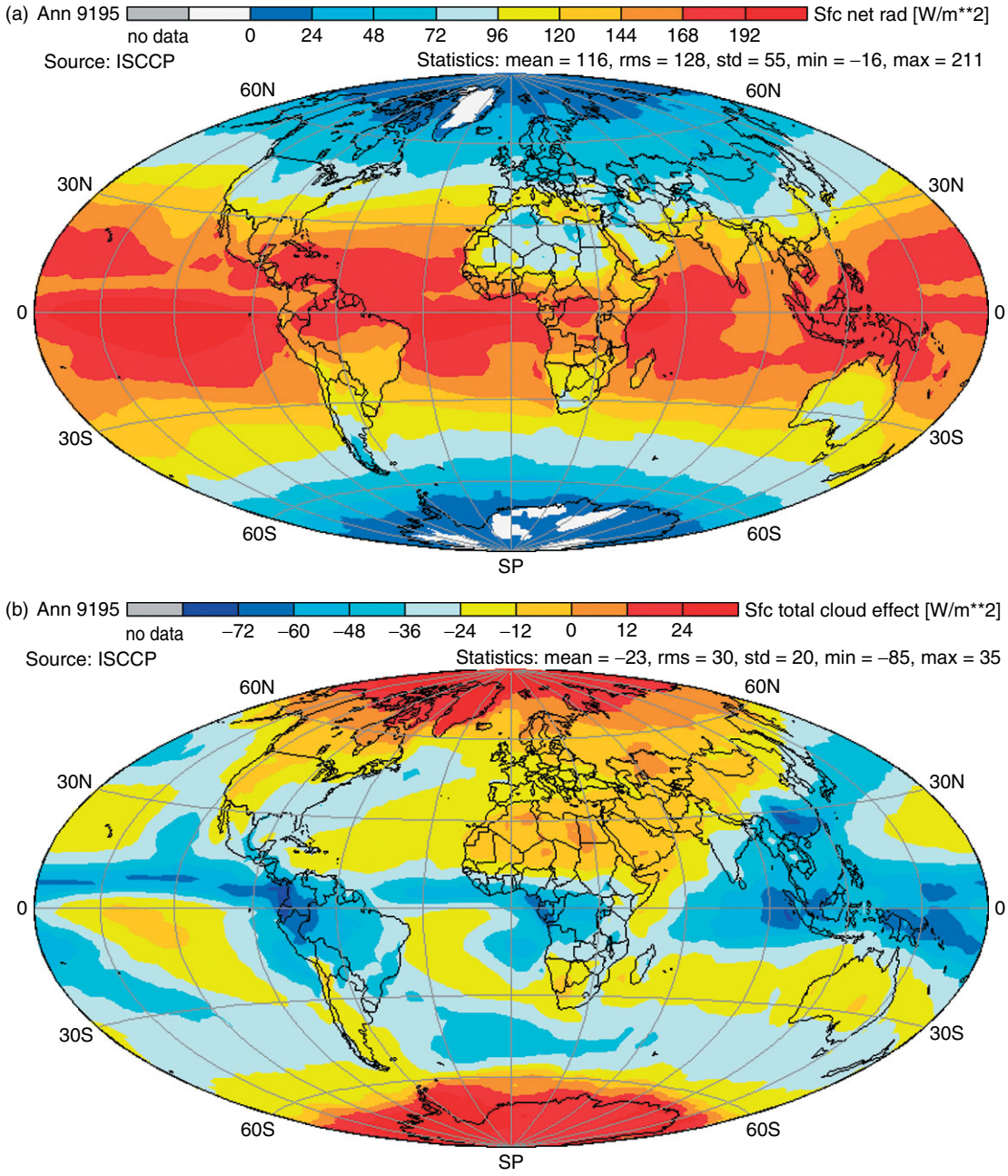

Figure 7. (a) Total net radiation at the ground and (b) the cloud effects (cloudy–clear) on total net radiation during the period 1991 to 1995. Note the strong cloud effect of more than -60 W m^{-2} over southern China and over the tropical zone with well-known highest topped convective clouds

radiation in Figure 8(b) of the cloud contribution to the vertical flux divergence of solar radiation. The persistent low-level maritime stratocumulus fields contribute only relatively small amounts between about 30 and 42 W m^{-2} to the downward atmospheric radiation.

In Figure 7(a) and (b) we show the global maps of the annual total net radiation at the ground and of the cloud effects on it. These values represent now the sum of the solar and terrestrial radiation budgets at the ground.

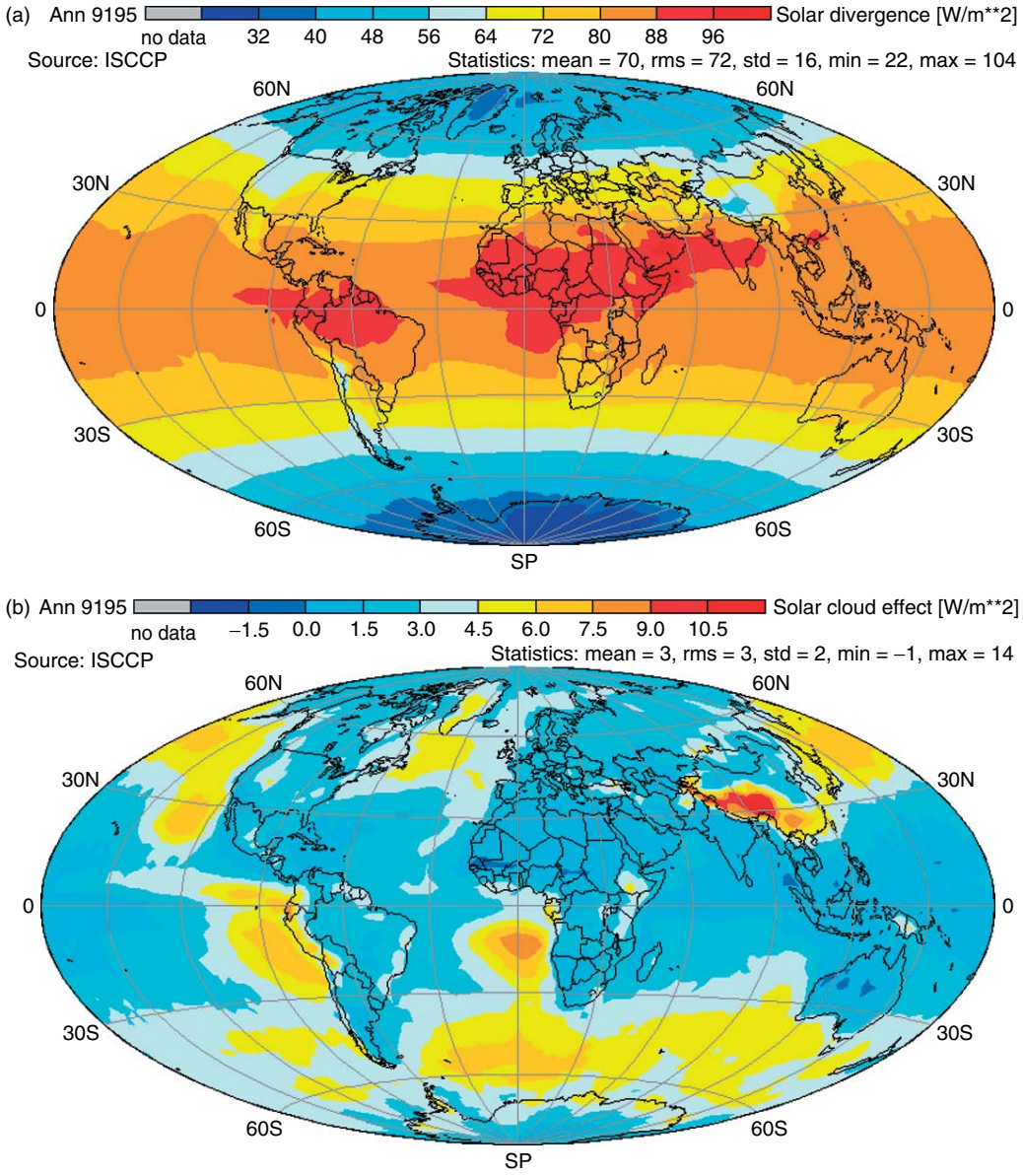

Figure 8. (a) Vertical divergence of solar radiation within the atmosphere, as computed from the ISCCP-FD data set (1991–95). Note the strong regional minima over the Highland of Tibet, north of Nepal, and over the Andes. (b) The effect of clouds (cloudy–clear) on the divergence of solar radiation within the atmosphere (1991–95). Positive values in this case mean that the net effect of clouds is to enhance the total column absorption by small amounts (in these multi-annual averages); however, they simultaneously reduce by reflection the total amount, available for absorption, and the absorption in atmospheric layers below them

As expected, almost everywhere on the globe the total radiation budget at the ground is positive, with the highest values over the tropical oceans (lowest surface albedo and highest temperature in the lower troposphere) and with lowest (negative to -15 W m^{-2}) values over both polar regions. These small 'negative' areas over the Greenland ice and over the Antarctic continent might be caused by errors in the retrieved cloud characteristics, but they could also correctly indicate net heating of the surface on average by occasional advection of warm, moist, cloudy air over these high-attitude locations. Smaller values of less than about 96 W m^{-2} also occur over the dry continental regions in the subtropics.

In general, clouds (Figure 7(b)) tend to *increase* slightly the gain of radiative energy over both polar regions up to amounts of about 30 W m^{-2}. Otherwise, at the present climate state, these areas would radiatively cool off more than now. Similar values were also found by Pavolonis and Key (2003), who analysed an earlier version of ISCCP data and data from the NOAA Polar Pathfinder Project. Walsh and Chapman (1998) also documented an arctic cloud–radiation–temperature association, which has been observed but was not reproduced in re-analyses at that time.

Elsewhere on the globe, clouds *decrease* the radiation budget at the surface in comparison with the clear atmosphere due to their overwhelming decrease of downward transmission of solar radiation where clouds decrease. The largest reductions of the clear-sky radiation budget by clouds (due to their high reflectance to space) occur over the areas of strong convective activity in the tropics, and again over southern China, with values of up to 75 W m^{-2}, which correspond almost to 40–50% of the clear-sky budget. The aforementioned maritime stratocumulus fields can often reduce the radiation budget at the ground by more than 60 W m^{-2} due to their high reflectance, which is only partly compensated by downward emission from their low (and relatively warm) cloud bases. A relatively small cloud effect has been found again over the dry subtropical continental regions, where even some areas of small increase occur. This small increase might be due to the presence of optically very thin (e.g. cirrus or level stratiform cumuli) clouds, which enhance only extremely slightly the reflectance to space but increase the downward terrestrial radiation.

4.3. Gain and loss of radiant energy by the atmosphere (vertical divergence)

The gain/loss of radiant energy by the atmosphere (also called vertical radiative flux divergence) is computed from the difference between the net flux densities at the TOA and at the ground, since the solar radiation incident at the TOA is the only external energy source and is, therefore, counted as positive. Positive (negative) differences mean net gain (net loss) of radiative energy by the atmosphere. Thus, positive values actually describe a convergence (i.e. negative divergence) within the atmosphere, which is indeed a gain of radiative energy, and negative values mean a net loss of radiative energy to space and/or towards the ground.

We felt it worth computing this difference between two often relatively large quantities with already high uncertainty range of about 5 to 10 W m^{-2}, despite the possibility of resulting systematic errors in the range of about 10 to 20 W m^{-2}, and to discuss the cloud effects on them. In this case, the ISCCP-FD calculations are physically consistent calculations using the same set of physical quantities, so that the errors are somewhat less than the sum of the separate errors (see discussion in Zhang *et al.* (1995)). In fact, interesting spatial patterns are found (shown in Figure 8(a) and (b)) that need further detailed explanation. Only a more rigorous assessment of the net fluxes at the TOA and at the ground than now can help reduce the uncertainty in values of the vertical flux divergence. Such work is now under way within the GEWEX framework.

The pattern in the map of the vertical divergence of solar radiation (Figure 8(a)) is overwhelmingly caused by the meridional gradients of the annual mean incident solar radiation. Clouds and high elevated continental areas cause only relatively small anomalies in the dominating zonal pattern over the tropical and subtropical areas. The largest gains of radiative energy in the equatorial belt are mostly related to the high amounts of atmospheric water vapour. The values here might be too small by 10 to 15 W m^{-2}, since the 'ISCCP atmosphere' was found to be somewhat too transparent for solar radiation (see Figure 4).

Clouds, Figure 8(b), generally increase the absorption of solar radiation within the atmosphere. We find everywhere in Figure 8(b), except for a few spots over tropical Africa and over Australia, small but positive values for the cloud effect on the solar divergence. These relatively low values can also be explained by several compensating effects. (1) Clouds reflect relatively large amounts of solar radiation back to space and transmit relatively small amounts to ground; thus they reduce considerably the absorption by water vapor in lower tropospheric layers below the clouds. (2) Clouds, and the water vapour in them, absorb more sunlight than just the water vapour in their layers alone. (3) Some of the reflected sunlight is absorbed on its second passage through the ozone layer and the water vapour above clouds (this is a smaller effect). The occasional small negative values are not errors; rather, they are examples of where the absorption in the cloud layer is not sufficient to offset the reduced absorption by water vapour below the cloud, which can happen even for high thin clouds in moist atmospheres. Further, we must assume on the basis of the comparisons with

ground-based measurements of downward solar radiation shown in Figure 4, that the 'ISCCP atmosphere' is more transparent for solar radiation than reality because of too small an aerosol absorption. These uncertainties indeed call for more worldwide comparisons of measured and satellite-derived fields of the downward solar and terrestrial radiation fluxes. The divergence of solar radiation may increase in the tropical and subtropical regions by 5 to 10 W m^{-2}. We consider the above-mentioned few spots with negative values in Figure 8(b) as errors in our computational procedure. No account in this study can be given to the role of additional aerosols, which are not considered completely in the computational procedure. They might, as observed for thin cirrus over snow fields, increase the absorption over highly reflecting surfaces.

The largest enhancement of absorption by clouds can be found over the Highland of Tibet and southwestern China, where the high topography removes the absorption by water vapour at lower levels that offsets the added cloud absorption in most other locations. Other, but smaller, maxima occur over the central portions of the aforementioned maritime stratocumulus fields and the major storm track regions at mid-latitudes over the oceans.

Clouds, therefore, enhance only by relatively small amounts the absorption of solar radiation by the total atmospheric column. The values obtained from the ISCCP-FD data set might be somewhat too small (by possibly 3 to 10 W m^{-2}), since we have already diagnosed that the ISCCP algorithm might give low results, since the treatment of aerosols is incomplete.

This data set is not suited to confirm or refute the 'anomalous high absorption' of solar radiation within clouds, which has been the subject of intensive investigation during the past 5 to 10 years (see conclusive discussion by Li *et al*. (2003)).

The divergence of terrestrial radiation within the atmosphere is negative everywhere on the globe (Figure 9(a)), as is known. The largest losses of more than (−) 235 W m^{-2} are found over the eastern portions of the South Pacific and Atlantic Oceans due to the emission of relatively low, and therefore warm, cloud tops (Figure 9(b)). The high convective clouds over the ITCZ and within the major storm tracks reduce this cooling considerably. The smallest values of the cooling occur over the highest elevations of continents, due to the fact that their thinner atmospheres contain much less water vapour.

The amounts and spatial pattern of the net flux divergence and of the cloud contribution to it, as shown in Figure 10(a) and (b), is dominated by the contributions of terrestrial (IR) radiation due to the small enhancement of absorption of solar radiation by clouds. We find the largest losses of radiative energy over both aforementioned areas known to be covered with persistent low marine stratocumulus decks with only few higher cirrus elements on top, but losses are also relatively high, more than 110 W m^{-2}, over southern China and over many parts of the world oceans, and interestingly near the Arctic sea ice. This intensive radiative cooling must indeed be compensated by vertical heat transport from the ground and by horizontal transports by the atmospheric circulation (the former more at low latitudes and the latter more at higher latitudes). The smallest values are found over Central Africa, due to the very high input of solar radiation, and over the high elevated central Asian desert regions, over Western Australia and the southern portion of South America.

This pattern is dominated by the orography of the continents and the related thickness of the atmosphere. But, over the eastern part of the Indian Ocean and the western part of the Pacific these smaller values of loss of radiative energy are caused by the deep convective cloud systems.

We also computed the ratio $R = CE_{sfc}/CE_{toa}$, of the cloud effects (CE) on the solar and terrestrial net radiation at the surface and at the TOA, following a suggestion by Li *et al*. (1995) and others. Knowing R, the cloud effect on the gain of the atmosphere (CE_{atm}) can be obtained from $CE_{atm} = (R - 1)CE_{toa}$. This ratio has been interpreted by Li *et al*. (1995), and in other sources, as a measure for the absorption of solar radiation by clouds, although a more careful interpretation also has to consider the forward and backward scattering events and the effects of water vapour and aerosols.

With the ISCCP-FD data this ratio has been found for the solar component everywhere on the globe with values larger than unity, but only up to values of 1.16, indicating that the absorption (in the sense of Li *et al*. (1995)) within the atmosphere might be much smaller than by the Earth–atmosphere system and that the cloud effect on downward solar radiation is everywhere higher than on the upward component. The spatial pattern is quite similar to that shown in Figure 8(b). Similar small values have also been computed by Wild (2000) in a study of the absorption of solar radiation in the atmosphere over Germany. In the IR this ratio is due to

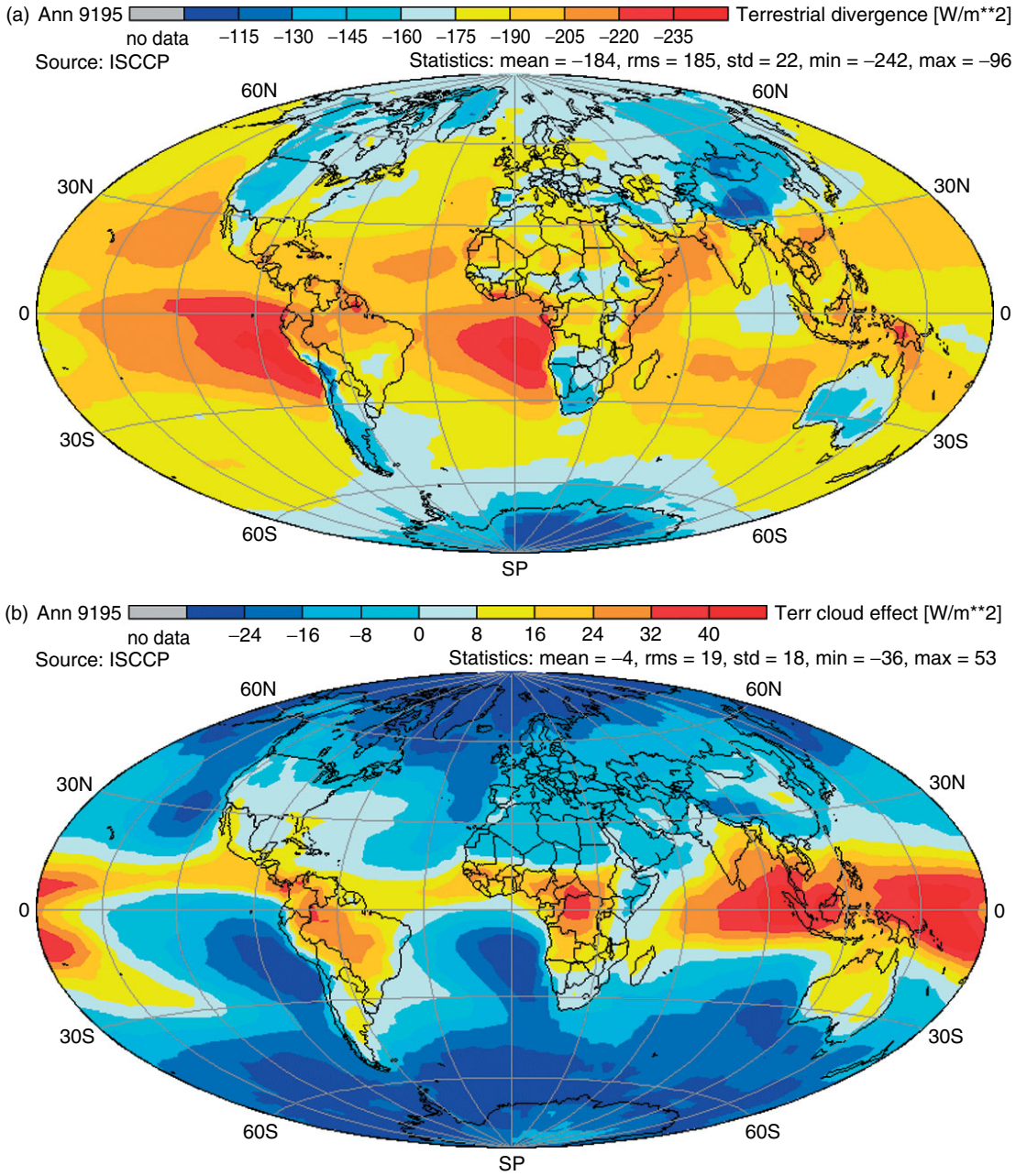

Figure 9. (a) Vertical divergence of terrestrial radiant energy (W m^{-2}) and (b) effects of clouds (cloudy–clear) on the vertical divergence of terrestrial radiant energy (W m^{-2}) during the period 1991 to 1995. Over all positive (negative) areas clouds enhance (reduce) the longwave divergence. The drastic reduction at higher latitudes is primarily caused by stronger cloud effects on downward atmospheric radiation, since much less water vapour is present in the lower troposphere than in the tropics

a very complex interaction between clouds, gaseous absorbers and other atmospheric properties and cannot, therefore, be easily interpreted in terms of cloud absorption. We find values of $R > 0$ everywhere, where values of $R > 1$ are obtained over all those regions where the cloud effect on the divergence of terrestrial radiation (Figure 9(b)) is negative (i.e. where clouds reduce the radiative cooling of the atmosphere). The spatial pattern is quite similar to that in Figure 9(b).

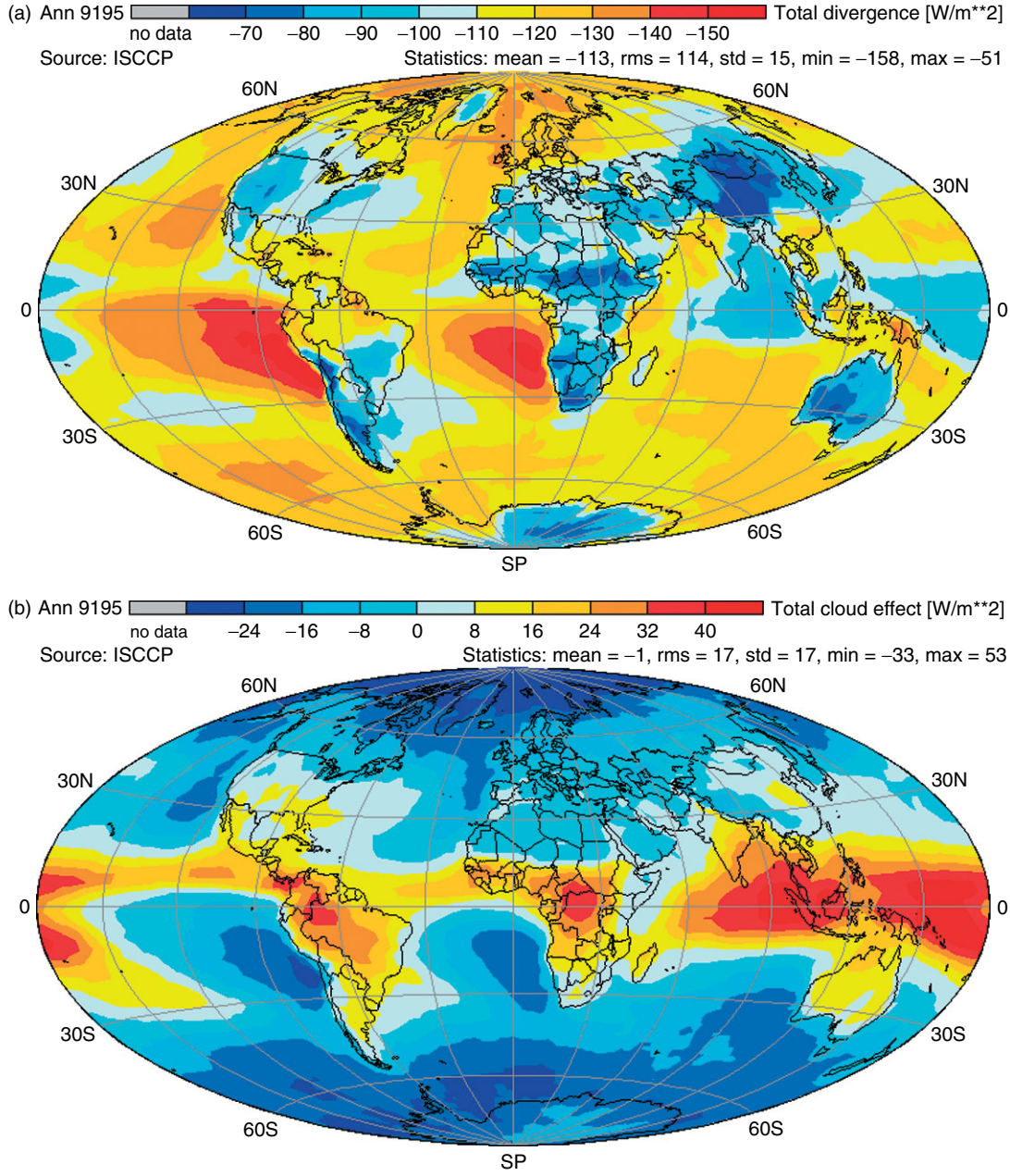

Figure 10. (a) Total radiative flux divergence (W m^{-2}) in the atmosphere and (b) effect of clouds (cloudy–clear) on radiative flux divergence (W m^{-2}) during the period 1991 to 1995. (a) The atmosphere generally loses radiative energy, which is compensated by turbulent fluxes of latent and sensible heat from below. (b) Positive (negative) values mean that clouds reduce (enhance) the loss of radiative energy within the atmosphere. We find the largest reductions over the ITCZ, which are often covered with deep convective cloud systems

5. SUMMARY DISCUSSION

We begin this discussion with the previously made explanation that this ISCCP-radiation budget is the result of radiative transfer calculations with the GISS radiation code and with ISCCP cloud and correlative data sets (see Table I) as input. Space-borne measurements of the radiation budget at the TOA and ground-based

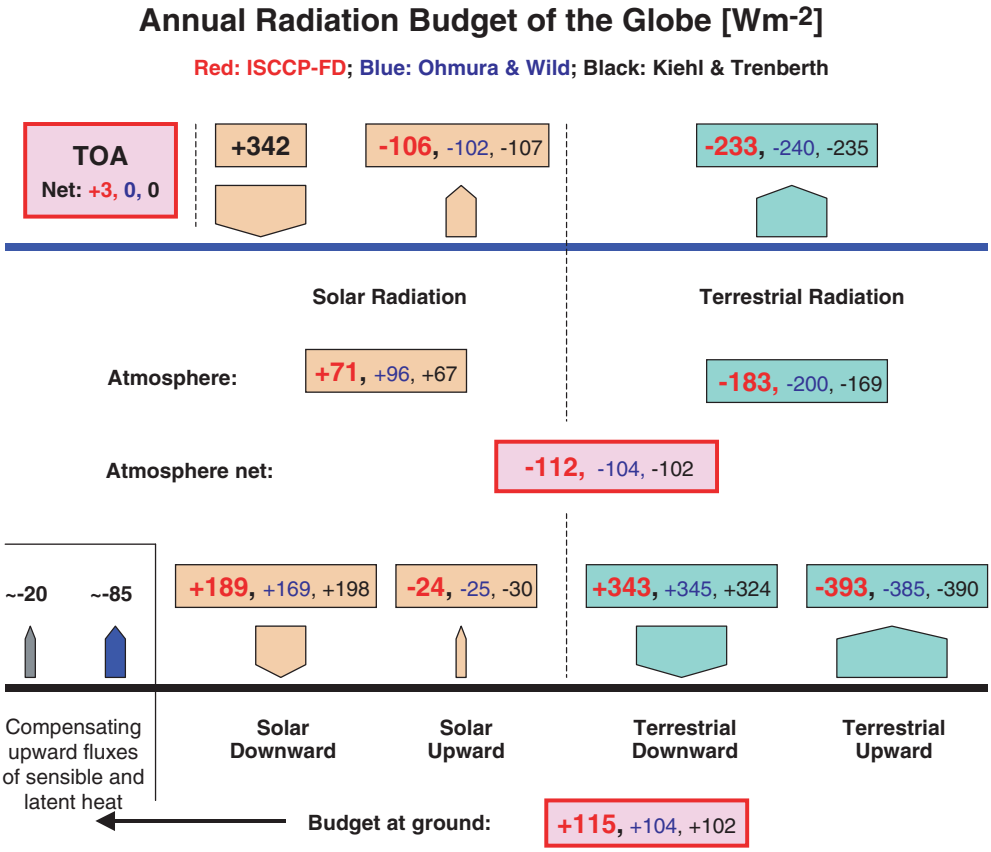

Figure 11. Annual radiation budget of the climate system (W m^{-2}) calculated from the ISCCP data set (red numbers) and compared with results from Ohmura and Wild (blue numbers) and Kiehl and Trenberth (black numbers). The respective values for the total flux divergence in the atmosphere are -112 W m^{-2}, -104 W m^{-2} and -102 W m^{-2} respectively

Table IV. Effective values of albedo and surface temperature. Values for the ISCCP-FD data set result from detailed calculations with model input (see text)

	ISCCP-FD	Ohmura and Wild (personal communication, 2003)	Kiehl and Trenberth (1997)
Effective surface albedo (%)	13	15	15
Effective values			
Surface temperature (°C)	15.2	14.0	14.9
Emittance	0.97 (integral)	1.0	1.0

measurements are used only for validation purposes. The annual global averages of the ISCCP-FD data set (red numbers) are compared in Figure 11 with (as examples of a variety of other data) results reported by Kiehl and Trenberth (1997; black numbers in Figure 11) and Ohmura and Wild (personal communications, 2003, blue numbers), which these authors compiled by combinations of satellite-based and ground-based climatologies. Table IV summarizes some complementary information on the effective albedo at the ground and on the effective values of the surface emittance and temperature. The surface albedo and emittance are naturally modelled in the analyses of ISCCP data with a high regional detail including angular dependencies, whereas the other workers 'forced' their budget estimates with prescribed averages of the global surface albedo and emittance.

The annual averages of the radiation budget components at the TOA of all three studies agree quite well within the error limits given in the right column of Table V. Larger differences between these three data sets are found for the budgets at the ground, where Ohmura and Wild (Personal communication, 2003) seem to overestimate the absorption of solar radiation within the atmosphere relative to the other estimates. The atmosphere of Kiehl and Trenberth (1997) seems to emit less to the ground than in the other two data sets. Their terrestrial divergence is almost 10 to 15% smaller than the others.

At the ground, however, the values by Ohmura and Wild (Personal communication, 2003) for the downward solar and those by Kiehl and Trenberth (1997) for the downward terrestrial radiation are much lower than the ISCCP-FD values (by about 20 W m^{-2}). These differences cause further differences in the values of the net radiation and, consequently, also in the radiative flux divergence. Values of the effective surface temperature in the ISCCP results are based on the input data mentioned at the beginning and represent the emitting (skin) temperature of the solid or liquid surface. Ohmura and Wild (Personal communication, 2003) normalized their data to the mean atmospheric temperature at ground of 14 °C given by Jones *et al*. (1999) and Kiehl and Trenberth (1997) normalized to an earlier global average of about +15 °C.

The lower effective surface albedo values of the ISCCP-FD (these are multi-annual averages of daily sums) are caused by several assumptions on the ocean albedo and its dependence on the solar zenith angle, and also on the sea-ice and snow distributions entering these calculations. Note that if the CERES data are correct (Figure 2) then they imply an even lower surface albedo and an even higher surface temperature than inferred by ISCCP-FD.

Table V summarizes the global averages for all computed quantities and also adds conservative estimates of uncertainty ranges. These latter values are based on the error discussion in previous work (Zhang *et al*., 1995, 2004). It further shows the seasonal variability of these global averages, which in part is due to the seasonal insolation and to the non-symmetric distribution of continents over both hemispheres of our globe.

Table VI summarizes for the sake of completeness the global averages of the radiative flux divergences (lowest three lines) and of the clouds effects on all budget parameters. For the fluxes at the TOA the ISCCP-based calculations yielded values similar to those estimated from the measurements of the ERBE (e.g. Barkstrom, 1984), amounting to +32 W m^{-2}, −49 W m^{-2} and −17 W m^{-2} respectively. About one-half of the planetary albedo can be attributed to clouds. The ISCCP data sets also allow estimates of the cloud effects on budgets at the ground and within the atmosphere itself. No comparison of these global values with results

Table V. Global annual and seasonal averages of the ISCCP-FD radiation budget during the period 1991 to 1995. The right column also gives rough estimates of uncertainties (more detail is discussed in the text). The seasonal variation of all quantities can, in part, be explained by the Earth's orbit around the sun and by the different land–sea distribution in both hemispheres

Quantity	Annual	DJF	MAM	JJA	SON	Estimated uncertainty range
Incident solar radiation at TOA (W m^{-2})	342	352	340	332	334	±0.25
Reflected solar radiation at TOA (W m^{-2})	−106	−112	−105	−101	−108	±5–7
Solar radiation absorbed at TOA (W m^{-2})	236	240	235	231	236	±5–7
Planetary albedo (%)	31	32	31	30	32	±1
Outgoing terrestrial radiation at TOA (W m^{-2})	−233	−231	−232	−236	−233	±3–5
Radiation budget at TOA (W m^{-2})	+3	+9	+3	−5	+3	±5–7
Downward solar radiation at ground (W m^{-2})	189	195	190	180	190	±7–10
Net solar radiation at ground (W m^{-2})	165	169	165	160	167	±7–10
Downward terrestrial radiation at ground (W m^{-2})	343	335	342	351	342	±15–20
Net terrestrial radiation at ground (W m^{-2})	−50	−49	−51	−49	−50	±15–20
Total net radiation at ground (W m^{-2})	115	120	114	111	117	±15–20
Total radiative flux divergence (W m^{-2})	−112	−111	−111	−116	−114	±20
Solar radiative flux divergence (W m^{-2})	71	71	70	71	69	±15
Terrestrial radiative flux divergence (W m^{-2})	−183	−182	−181	−187	−183	±20

Table VI. Annual global averages of the effects of clouds (cloudy–clear) on various radiation budget components at the TOA and at the surface (SFC) and on the divergence within the atmosphere, discussed above, and of the divergences of radiation (lowest three lines)

Parameter	Annual	Dec–Feb	Mar–Apr	Jun–Aug	Sep–Nov
TOA: terrestrial cloud effect (W m^{-2})	+25	+25	+26	+25	+25
TOA: solar cloud effect (W m^{-2})	−50	−53	−46	−50	−50
TOA: total cloud effect (W m^{-2})	−24	−28	−20	−22	−26
SFC: terrestrial cloud effect (W m^{-2})	+30	+31	+30	+28	+30
SFC: solar cloud effect (W m^{-2})	−52	−57	−49	−50	−53
SFC: total cloud effect (W m^{-2})	−23	−26	−20	−21	−24
Cloud effect on terrestrial divergence (W m^{-2})	−4.3	−5.4	−3.5	−3.2	−5.3
Cloud effect on solar divergence (W m^{-2})	+3.0	+3.3	+2.7	+2.7	+3.2
Cloud effect on total divergence (W m^{-2})	−1.3	−2.1	−0.8	−0.5	−2.1

of other studies is possible yet, but one should at least compare regional values over continental areas with well-maintained ground-based radiation networks.

6. FINAL REMARKS

We have presented some first results from the ISCCP on the annual radiation budget components of the atmosphere at both of its boundaries and emphasized the effect of clouds on them. Possibly for the first time, global maps of the gain or loss of radiant energy within the atmosphere (vertical radiative flux divergence) are also shown. Patterns in all maps have reasonable explanations on the basis of the presence of clouds and of their mean altitude. Of particular interest are 'anomalies' in almost all fields over Southeast Asia and the maritime near-coastal stratocumulus fields.

Some of these patterns might also be caused by systematic biases in some of the data. In particular, it was found that in the tropics and subtropics the 'ISCCP atmosphere' is too transparent for solar radiation and the present results may underestimate the absorption within the atmosphere by about 10 to 20 W m^{-2}. The identification of cloud and the relatively high uncertainties in atmospheric and surface properties used over both polar regions might also be an important error source over both poles. In particular, the apparent long-term trends of Arctic haze, which are frequently reported (e.g. Sharma *et al*., 2004), should be taken into account in future computations of the surface radiation budget.

The values of the annual global budgets at the TOA obtained from the ISCCP data set and by Ohmura and Wild (personal communications, 2003) and Kiehl and Trenberth (1997) are in quite good agreement within a range of ±3–4 W m^{-2}. However, larger discrepancies (see Figure 11) occur within the budgets at the ground, leading to discrepancies in the solar and terrestrial radiation divergences, which need further investigation. One way is possibly a thorough assessment of all available data sets on the radiation budget at the TOA and at the ground and also on the cloud field properties as deduced from the ISCCP radiances.

ACKNOWLEDGEMENTS

We want to thank several organizations from the USA (National Aeronautics and Space Administration, National Oceanographic Atmospheric Administration, Colorado State University), from Canada (Meteorological Service of Canada), Japan (Japanese Meteorological Agency), France (Meteorologie National) and all European weather services (members of the EUMETSAT organization) for their steady contributions of data and resources to ISCCP during about the past 20 years. E.R. began this work in fall 2002 while visiting the Center of Climate System Research at the University of Tokyo, Japan. We also thank two anonymous reviewers whose critical and constructive suggestions helped to improve several portions of the original manuscript.

REFERENCES

Barkstrom BR. 1984. The Earth Radiation Budget Experiment (ERBE). *Bulletin of the American Meteorological Society* **65**: 1170–1186.
Betts AK, Beljaars ACM. 2003. ECMWF ISLSCP-II near-surface data set from ERA-40. ECMWF — ERA-40 Project Report Series No. 8, 31 pp
Brest CL, Rossow WB. 1992. Radiometric calibration and monitoring of NOAA AVHRR data for ISCCP. *International Journal of Remote Sensing* **13**: 235–273.
Brest CL, Rossow WB, Roiter MD. 1997. Update of radiance calibrations for ISCCP. *Journal of Atmospheric and Oceanographic Technology* **14**: 1091–1109.
Chen T, Rossow WB. 2002. Determination of top-of-atmosphere longwave radiative fluxes: a comparison between two approaches using ScaRab data. *Journal of Geophysical Research* **107**: (D84070). DOI: 10.1029/2001JD000914.
Covey C, Achuta Rao KM, Cubasch U, Jones P, Lambert SJ, Mann ME, Phillips TJ, Taylor WE. 2003. An overview of results from the Coupled Model Intercomparison Project. *Global and Planetary Change* **769**: 1–31.
Desormeaux Y, Rossow WB, Brest CL, Campbell GG. 1993. Normalization and calibration of geostationary satellite radiances for ISCCP. *Journal of Atmospheric and Oceanographic Technology* **10**: 304–325.
Gates WL, Boyle JS, Covey C, Dease CG, Doutriaux CM, Drach RS, Fiorino M, Gleckler PJ, Hnilo JJ, Marlais SM, Phillips TJ, Potter GL, Santer BD, Sperber KR, Taylor KE, Williams DN. 1999. An overview of the results of the Atmospheric Model Intercomparison Project (AMIP). *Bulletin of the American Meteorological Society* **80**: 29–55.
Gilgen H, Ohmura A. 1999. The global energy balance archive. *Bulletin of the American Meteorological Society* **80**: 831–850.
Hartmann DL, Doelling D. 1991. On the net radiative effectiveness of clouds. *Journal of Geophysical Research* **96**: 869–891.
Jin Y, Rossow WB, Wylie DP. 1996. Comparison of the climatologies of high-level clouds from HIRS and ISCCP. *Journal of Climate* **9**: 2850–2879.
Jones PD, New M, Parker DE, Martin S, Rigor IG. 1999. Surface air temperature and its changes over the past 150 years. *Reviews of Geophysics* **37**: 173–198.
Kiehl JT, Trenberth KE. 1997. Earth's annual global mean energy budget. *Bulletin of the American Meteorological Society* **78**: 197–199.
Li Z, Ackerman TP, Wiscombe W, Stephens GL, Kerr RA. 2003. Have clouds darkened since 1995? *Science* **302**: 1150–1151.
Li Z, Barker H, Moreau L. 1995. The variable effect of clouds on atmospheric absorption of solar radiation. *Nature* **376**: 486–490.
Mahesh A, Gray MA, Palm SP, Hart WD, Spinhirne JD. 2004. Passive and active detection of clouds: comparisons between MODIS and GLAS observations. *Geophysical Research Letters* **31**: L04108. DOI: 10.1029/2003GL018859.
Ohmura A, Dutton E, Forgan B, Fröhlich C, Gilgen H, Hegner H, Heimo A, König-Langlo G, McArthur B, Müller G, Philipona R, Pinker R, Whitlock CH, Dehne K, Wild M. 1998. Baseline surface radiation network (BSRN/WCRP): new precision radiometry for climate research. *Bulletin of the American Meteorological Society* **79**: 2115–2136.
Pavolonis MJ, Key JR. 2003. Antarctic cloud radiative forcing at the surface estimated from AVHRR polar pathfinder and ISCCP D1 datasets 1985 to 1993. *Journal of Applied Meteorology* **42**: 827–840.
Peixoto JP, Oort AH. 1992. *Physics of Climate*. American Institute of Physics: New York.
Randall D, Krueger S, Bretherton C, Curry J, Duinkerke P, Moncrieff M, Ryan B, Starr D, Miller M, Rossow W, Tselioudis G, Wielicki B. 2003. Confronting models with data — the GEWEX cloud systems study. *Bulletin of the American Meteorological Society* **84**: 455–469.
Raschke E. 1972. Die Strahlungsbilanz der Systems Erde–Atmosphäre — neuere Ergebnisse von Satellitenmessungen. *Zeitschrift für Geophysik* **38**: 967–1000.
Raschke E, Flamant P, Fouquart Y, Hignett P, Isaka H, Jonas PR, Sundqvist H, Wendling P. 1998. Cloud–radiation studies during the European Cloud and Radiation Experiment (EUCREX). *Surveys in Geophysics* **19**: 89–138.
Rossow WB, Cairns B. 1995. Monitoring changes of clouds. *Climatic Change* **31**: 305–347.
Rossow WB, Duenas L. 2004. The International Satellite Cloud Climatology Project (ISCCP) Web site — an online resource for research. *Bulletin of the American Meteorological Society* **85**: 167–172.
Rossow WB, Garder LC. 1993. Cloud detection using satellite measurements of infrared and visible radiances for ISCCP. *Journal of Climate* **6**: 2341–2369.
Rossow WB, Schiffer RA. 1991. ISCCP cloud data products. *Bulletin of the American Meteorological Society* **72**: 2–20.
Rossow WB, Schiffer RA. 1999. Advances in understanding clouds from ISCCP. *Bulletin of the American Meteorological Society* **80**: 2261–2287.
Rossow WB, Zhang Y-C. 1995. Calculation of surface and top-of-atmosphere radiative fluxes from physical quantities based on ISCCP datasets. Part II: validation and first results. *Journal of Geophysical Research* **100**: 1167–1197.
Rossow WB, Walker AW, Beuschel D, Roiter M. 1996. International Satellite Cloud Climatology Project (ISCCP) description of new cloud datasets. WMO/TD-No.737, World Climate Research Programme (ICSU and WMO), Geneva.
Schiffer RA, Rossow WB. 1983. The International Satellite Cloud Climatology Project (ISCCP): the first project of the World Climate Research Programme. *Bulletin of the American Meteorological Society* **64**: 779–784.
Schiffer RA, Rossow WB. 1985. ISCCP global radiance data set: a new resource for climate research. *Bulletin of the American Meteorological Society* **66**: 1498–1505.
Scott NA, Chédin A, Armante R, Francis J, Stubenrauch CJ, Chaboureau J-P, Chevallier F, Claud C, Chéruy F. 1999. Characteristics of the TOVS pathfinder path-B dataset. *Bulletin of the American Meteorological Society* **80**: 2679–2701.
Sharma S, Lavoue D, Cachier H, Barrie LA, Gong SL. 2004. Long-term trends of the black carbon concentrations in the Canadian Arctic. *Journal of Geophysical Research* **109**: (D15203). DOI: 10.1029/2003JD004331.
Smith WL, Woolf HM, Hayden CM, Wark DQ, McMillin LM. 1979. The TIROS Operational Vertical Sounder. *Bulletin of the American Meteorological Society* **60**: 117–118.
Seze G, Rossow WB. 1991. Effects of satellite data resolution on measuring the space/time variations of surfaces and clouds. *International Journal of Remote Sensing* **12**: 921–952.
Stephens GL, Vane DG, Boain RJ, Mace GG, Sassen K, Wang Z, Illingworth AJ, O'Connor EJ, Rossow WB, Durden SL, Miller SD, Austin RT, Benedetti A, Mitrescu C. The Cloudsat Science Team. 2002. The Cloudsat Mission and the A-Train — a new dimension of space-based observations of clouds and precipitation. *Bulletin of the American Meteorological Society* **83**: 1771–1790.

Stubenrauch CJ, Rossow WB, Cheruy F, Chedin A, Scott NA. 1999a. Clouds as seen by satellite sounders (3I) and imagers (ISCCP). Part I: evaluation of cloud parameters. *Journal of Climate* **12**: 2189–2213.

Stubenrauch CJ, Rossow WB, Scott NA, Chedin A. 1999b. Clouds as seen by satellite sounders (3I) and imagers (ISCCP): III combining 3I and ISCCP cloud parameters for better understanding of cloud radiative effects. *Journal of Climate* **12**: 3419–3442.

Valero FPJ, Pope SK, Bush BC, Nguyen Q, Marsden D, Cess RD, Simpson-Leitner AS, Bucholtz A, Udelhofen PM. 2003. Absorption of solar radiation by the clear and cloudy atmosphere during the Atmospheric Radiation Measurement Enhanced Shortwave Experiments (ARESE) I and II: observations and models. *Journal of Geophysical Research* **108**(D1): 4016. DOI: 10.1029/2001JD001384.

Walsh JE, Chapman WL. 1998. Arctic cloud–radiation–temperature associations in observational data and atmospheric reanalyses. *Journal of Climate* **11**(11): 3030–3045.

Wang J, Rossow WB, Zhang Y. 2000. Cloud vertical structure and its variations from a 20-yr global rawinsonde dataset. *Journal of Climate* **13**: 3041–3056.

Wielicki BA, Cess RD, King MD, Randall DA, Harrison EF. 1995. Mission to planet Earth: role of clouds and radiation in climate. *Bulletin of the American Meteorological Society* **76**: 2125–2152.

Wielicki BA, Barkstrom BR, Harrison EF, Lee RB, Smith GL, Cooper JE. 1996. Clouds and the Earth's Radiant Energy System (CERES): an earth observing system experiment. *Bulletin of the American Meteorological Society* **77**: 853–868.

Wild M. 2000. Absorption of solar energy in cloudless and cloudy atmospheres over Germany and in GCMs. *Geophysical Research Letters* **27**: 959–962.

Wylie DP, Menzel WP. 1999. Eight years of high cloud statistics using HIRS. *Journal of Climate* **12**: 170–184.

Yu R, Wang B, Zhou T. 2004. Climate effects of the deep continental stratus clouds generated by the Tibetan Plateau. *Journal of Climate* **17**: 2702–2713.

Zhang Y-C, Rossow WB, Lacis AA. 1995. Calculation of surface and top-of-atmosphere radiative fluxes from physical quantities based on ISCCP datasets. Part I: method and sensitivity to input data uncertainties. *Journal of Geophysical Research* **100**: 1149–1165.

Zhang Y-C, Rossow WB, Lacis AA, Oinas V, Mishchenko MI. 2004. Calculation of radiative flux profiles from the surface to top-of-atmosphere based on ISCCP and other global datasets: refinements of the radiative transfer model and the input data. *Journal of Geophysical Research* **109**: (D19105). DOI: 101029/2003JD004457.

